Available online at www.sciencedirect.com

ScienceDirect

IFAC PapersOnline CONFERENCE PAPER ARCHIVE

IFAC PapersOnLine 51-29 (2018) 450–456

Roll damping of a surface effect ship with split air cushion

Jonas Tønnessen * **Håkon E. Bryn** * **Jan T. Gravdahl** *
Vahid Hassani ** **Øyvind F. Auestad** ***

* *Department of Engineering Cybernetics, O. S. Bragstads plass 2D, NTNU, N-7491, Trondheim, Norway*
** *Department of Marine Technology, Otto Nielsens vei 10, NTNU, N-7491, Trondheim, Norway*
*** *Umoe Mandal AS, Gismeryveien 205, N-4515 Mandal, Norway*

Abstract: This paper considers linear modeling of a surface effect ship (SES) where roll motions are damped by exclusively exploiting a longitudinally split air cushion design. On a SES, the pressurized air cushions can support up to approximately 80 % of the vessels weight. By implementing a separating wall midships in the longitudinally direction, motion control of roll is possible. When the vessel is subject to wave-induced roll motions, the starboard and port air cushion pressures are controlled in anti-phase, reducing these motions significantly. The effectiveness of the scheme is demonstrated through model scale experimental testing carried out in the Towing Tank, NTNU, Trondheim. [1]

Keywords: Surface effect ship, Marine systems, Ship control, Roll damping

1. INTRODUCTION

1.1 Further offshore - rougher sea conditions

The current trend in the offshore wind industry, is that the turbines are located further from shore and in deeper waters as seen from Figure 1. As a direct result of this, Crew Transfer Vessels (CTVs) encounter rougher sea-conditions. The case studied in this article is the WAVECRAFT^{TM} which is a surface effect ship (SES) CTV. The WAVECRAFT^{TM} is already supplied with heave and pitch damping (Auestad et al., 2015). The contribution of the work presented in this paper is to modify the air cushion setup and design a controller that reduces roll motions on the WAVECRAFT^{TM}. By including a roll damping control system, all degrees of freedom in the vertical plane can be damped.

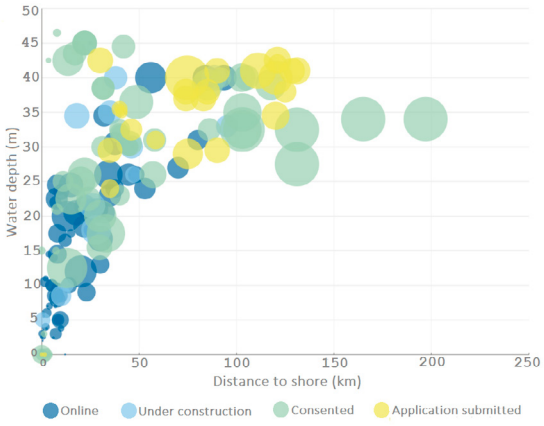

Fig. 1. Wind farms: water depth and distance to shore (WindEurope, 2017).

1.2 SES design

A surface effect ship (SES) is a marine craft with catamaran hull, equipped with flexible seal systems at the bow and stern. The air cushion is defined as the enclosed volume between the hull, seals and water plane as seen in Figure 2. The cushion is pressurized by lift fans, which supplies the air cushion with an air inflow. A SES is also equipped with variable vent valves, in order to control the air outflow from the cushion. Hence, the vent valves can be utilized to control the air cushion pressure. Figure 2 illustrates the conventional SES setup.

[1] This work was supported by Innovation Project for the Industrial Sector (IPN) 256442/O80 "SES service fartøy for vindmølleparker til havs" and was carried out in cooperation with Umoe Mandal AS, the Centre for Autonomous Marine Operations and Systems (AMOS), and SINTEF Ocean; the Norwegian research council is acknowledged as the main sponsor of AMOS and IPN 256442/O80.

10.1016/j.ifacol.2018.09.446

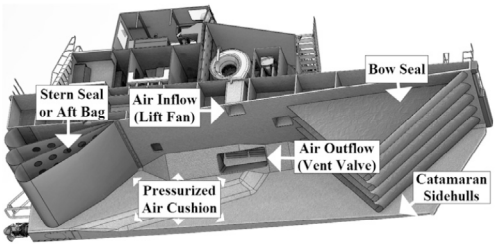

Fig. 2. SES concept (Courtesy of Umoe Mandal).

1.3 Air cushion control systems

Two major control regimes have been developed for SES, ride control systems (RCS) developed by among others Kaplan and Davis (1978), Adams et al. (1983) and Sørensen and Egeland (1995) and the boarding control system (BCS) developed by Auestad et al. (2015). The former reduces vertical accelerations experienced during transit at moderate to high vessel speeds, while the latter damps vertical bow accelerations at zero and low vessel speeds.

1.4 Roll damping systems

Today, both active and passive roll damping systems exist (Perez, 2005). An active system, like fin stabilizers, rudder roll damping and gyroscopic roll stabilizers, employs control surfaces or masses to induce a roll moment which counteracts wave-induced roll motions. Hull modifications are often performed to achieve passive roll damping, which does not require additional control (Fossen, 2011).

1.5 Separating wall implementation

For this project exclusively, the air cushion is divided longitudinally along the center-line by exploiting a flexible separating wall design. This is done in order to actively damp roll motions, exclusively by using the starboard and port air cushion pressure. The wall is flexible and pressurized by the bag fan, and thereby able to move lateral to some extent.

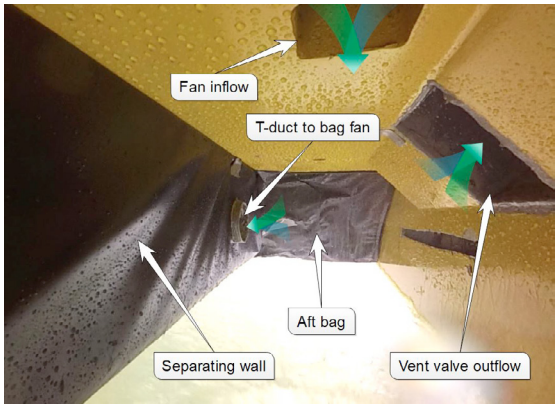

Fig. 3. Port air cushion of the current separating wall implementation.

The port air cushion for the model scale vessel is shown in Figure 3. It is seen that the flexible separating wall is fixed to the wetdeck and and aft bag. By design, the bottom part of the wall is always located below the water line during roll damping.

2. MATHEMATICAL MODELING

A linear control plant model (CPM), including the starboard and port pressure dynamics and the roll dynamics, is developed. This is a simplified mathematical model of a SES, which is employed for control system design and stability analysis. It contains the main physical properties of the pressure and roll dynamics. The CPM is expressed in the hydrodynamic frame as illustrated in Figure 4.

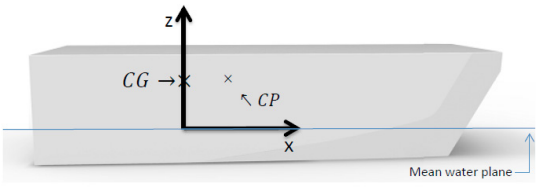

Fig. 4. Hydrodynamic frame. Illustration taken from Auestad et al. (2015).

The origin of the hydrodynamic frame is located at the mean water plane below the center of gravity (CG), and thereby follows the path of the vessel. The figure implies that the x, y and z axes are defined positive forward, to the port and upwards, respectively. The center of pressure (CP) denotes the point of attack for the pressure and is located at a transversely and longitudinally distance from CG, enabling motion control for roll and pitch, respectively.

For simplicity of the control design and stability analysis, the separating wall is considered to be fixed and therefore not able to move for the control plant model. Consequently, the air cushion areas, which is the mean water plane areas inside the cushions, are anticipated to be constant. Hence, the longitudinally lever arms between CG and CP are assumed equal for both cushions, while the transverse lever arms are assumed to be at opposite direction but same magnitude. This is an approximation made in order to reduce the complexity of the stability analysis. By design, the separating wall experience minor oscillations around the vertical position. However, this does not affect the control system design or the stability analysis and is therefore not considered here.

2.1 Control plant model

Linearized pressure dynamics For the CPM the starboard and port air cushion pressures are assumed uniform. The starboard and port air cushion pressure are expressed $p_i(t) = p_a + p_{u_i}(t)$ for $i = \{s, p\}$, where p_a and $p_{u_i}(t)$ are the atmospheric pressure and the excess air cushion pressures, respectively. The subscript s and p denote starboard and port, respectively. The air cushion pressure dynamics are linearized about an equilibrium pressure, p_0, which occurs for constant lift fan air flow, constant vent valve leakage areas and in the absence of waves. p_0 is assumed equal for both cushions.
A uniform, non-dimensional cushion pressure variation parameter is defined according to

$$\mu_{u_i}(t) = \frac{p_{u_i}(t) - p_0}{p_0}. \tag{1}$$

The volumetric air flows into the cushions, Q_{in_i}, are approximated by the fan characteristic curve which is a function of air cushion pressure. Leakages under the side hulls, separating wall and seals are assumed small and therefore not included in the control plant model. Therefore, it is assumed that the volumetric outflows through the identical vent valves are the only outflows out of the cushions and are written

$$Q_{out_i}(t) = c_n A_i^{ctrl}(t)\sqrt{\frac{2p_i(t)}{\rho_a}}, \tag{2}$$

where c_n is a vent valve coefficient determining the local shape of the vent valves. $A_s^{ctrl}(t)$ and $A_p^{ctrl}(t)$ are the variable leakage areas for the starboard and port vent valve, respectively. They are defined as

$$A_i^{ctrl}(t) = A_0^{ctrl} + \Delta A_i^{ctrl}(t), \tag{3}$$

where A_0^{ctrl} represents a mean operating value or bias opening that allows two sided control. $\Delta A_s^{ctrl}(t)$ and $\Delta A_p^{ctrl}(t)$ denote the controllable leakage areas for the starboard and port air cushion, respectively.
The uniform pressure equations are inspired by the work of Sørensen and Egeland (1995) and Auestad et al. (2015). A model for the starboard and port air cushion pressure dynamics are expressed in the hydrodynamic frame according to

$$\begin{aligned} &K_1\dot{\mu}_{u_i}(t) + K_3\mu_{u_i}(t) + \rho_{c0}A_c\dot{\eta}_3(t) \mp \rho_{c0}A_c y_{cp}\dot{\eta}_4(t) \\ &-\rho_{c0}A_c x_{cp}\dot{\eta}_5(t) = K_2\Delta A_i^{ctrl}(t) + \rho_{c0}\dot{V}_{0_i}(t), \end{aligned} \tag{4}$$

where

$$\begin{aligned} K_1 &= \frac{\rho_{c0}h_0A_c}{\gamma\left(1+\frac{p_a}{p_0}\right)} \\ K_2 &= \rho_{c0}c_n\sqrt{\frac{2p_0}{\rho_a}} \\ K_3 &= \frac{\rho_{c0}}{2}\left(Q_0 - 2p_0q\frac{\partial Q_{in}}{\partial P}\mid_0\right). \end{aligned} \tag{5}$$

The air densities ρ_a and ρ_{c0} occur for the atmospheric pressure p_a and the equilibrium pressure p_0, respectively. The air cushion area is denoted A_c. The air cushion height is expressed by h_0. The variables x_{cp} and y_{cp} are the longitudinal and transverse distances between CG and CP, respectively. The equilibrium air flow for the equilibrium pressure is denoted Q_0 and $\frac{\partial Q_{in}}{\partial P}\mid_0$ is the linearized lift fan characteristic slope at the equilibrium point, (p_0, Q_0). The ratio of specific heat for air is expressed by γ and the parameter q denotes the number of lift fans that are running at same frequency.
The heave displacement, $\eta_3(t)$, is the translation along the z axis. The roll angle, $\eta_4(t)$, and the pitch angle, $\eta_5(t)$, is rotation around the x and y axis, respectively.
The corresponding rates for these DOFs are denoted $\dot{\eta}_i(t)$ for $i = 3, 4, 5$. Positive translation and rotation are defined according to the right hand rule. Note that $\mp$ denotes $-$ and $+$ for the starboard and port cushion pressure, respectively. Since $Q_0 > 2p_0q\frac{\partial Q_{in}}{\partial P}\mid_0$ and all terms in Equation (5) have positive interpretation, it follows that $K1, K2, K3 > 0$.
The wave volume pumping, $\dot{V}_{0_i}(t)$, represents the rate of change of volume inside the cushion due to waves (Faltinsen, 2005). An equation for this variable is developed for the general case of various headings. The wave volume pumping is found by integrating the rate of change of the wave elevation, $\dot{\zeta}(x, y, t)$, longitudinally and transversely along the air cushions according to

$$\dot{V}_{0_i}(t) = \int_{-W_i(t)/2}^{W_i(t)/2}\int_{-L_i(t)/2}^{L_i(t)/2}\dot{\zeta}_i(x, y, t)\,dx\,dy, \tag{6}$$

where $L_i(t)$ and $W_i(t)$ are the length and width of the air cushions, respectively. The wave elevation is defined by Perez (2005) as

$$\zeta_i(x, y, t) = \bar{\zeta}\sin\Big(\omega t + \epsilon - k\big(x\cos(\chi) + y\sin(\chi)\big)\Big), \tag{7}$$

where $\bar{\zeta}$ is the constant wave amplitude, ω is the wave frequency, ϵ is the phase and χ is the direction the waves propagate with respect to the hydrodynamic frame, which makes the wave volume pumping valid for various wave directions. By differentiating the wave elevation with respect to time its rate of change is found as

$$\dot{\zeta}(x, y, t) = \bar{\zeta}\omega\cos\Big(\omega t + \epsilon - k\big(x\cos(\chi) + y\sin(\chi)\big)\Big). \tag{8}$$

Roll dynamics The differential equation for roll, dependent on the starboard and port cushion pressures, can according to Bryn and Tønnessen (2017) be written

$$\begin{aligned} &(I_{44} + A_{44})\ddot{\eta}_4(t) + B_{44}\dot{\eta}_4(t) + C_{44}\eta_4(t) \\ &+ y_{cp}A_cp_0\mu_{u_s}(t) - y_{cp}A_cp_0\mu_{u_p}(t) = F_4^e(t), \end{aligned} \tag{9}$$

where A_{44}, B_{44} and C_{44} represent the hydrodynamic added mass, potential damping and restoring coefficients for roll motion, respectively. $F_4^e(t)$ and I_{44} are the hydrodynamic wave excitation moment and moment of inertia for roll, respectively.

State-space model The starboard and port pressure dynamics and the roll dynamics in equation (4) and (9), respectively, are included in the control plant model which is written as an LTI state-space model

$$\begin{aligned} \dot{\boldsymbol{x}}(t) &= \boldsymbol{A}\boldsymbol{x}(t) + \boldsymbol{B}\boldsymbol{u}(t) + \boldsymbol{E}\boldsymbol{w}(t) \\ \boldsymbol{y}(t) &= \boldsymbol{C}\boldsymbol{x}(t), \end{aligned} \tag{10}$$

where the state vector, $\boldsymbol{x}(t)$, is defined in Table 1. Since only roll motion is considered, the heave and pitch motion influence on the pressure dynamics expressed in equation (4) is not considered for the CPM.

Table 1. Control plant model states.

State	Description	Notation
$x_1(t)$	Roll angle	$\eta_4(t)$
$x_2(t)$	Roll angular momentum	$(I_{44}+A_{44})\dot{\eta}_4(t)$
$x_3(t)$	Dynamic starboard cushion pressure	$\mu_{u_s}(t)$
$x_4(t)$	Dynamic port cushion pressure	$\mu_{u_p}(t)$

$\boldsymbol{u}(t) = \left[\Delta A_s^{ctrl}(t)\ \Delta A_p^{ctrl}(t)\right]^\top$,
$\boldsymbol{w}(t) = \left[F_4^e(t)\ \dot{V}_{0_s}(t)\ \dot{V}_{0_p}(t)\right]^\top$ and
$\boldsymbol{y}(t) = [\eta_4(t)\ \dot{\eta}_4(t)\ p_s(t)\ p_p(t)]^\top$ are the input, disturbance and measurement vector, respectively. The system matrix, $\boldsymbol{A}$, the input matrix, $\boldsymbol{B}$, the measurement matrix, $\boldsymbol{C}$, and the disturbance matrix, $\boldsymbol{E}$, are included in Appendix A.

3. CONTROL SYSTEM DESIGN

3.1 Control law

The control plant model expressed in equation (10) is employed for control system design and stability analysis. A proportional controller is evaluated in the stability analysis. For the stability analysis, the control law

$$\boldsymbol{u}(t) = -\boldsymbol{K}\boldsymbol{x}(t), \tag{11}$$

is investigated. The gain matrix, $\boldsymbol{K}$, is written

$$\boldsymbol{K} = \begin{bmatrix} 0 & k_{p_s} & 0 & 0 \\ 0 & -k_{p_p} & 0 & 0 \end{bmatrix}. \tag{12}$$

3.2 Stability analysis

The unperturbed closed-loop system, which do not include disturbances, can be written according to

$$\dot{\boldsymbol{x}}(t) = \boldsymbol{A}\boldsymbol{x}(t) + \boldsymbol{B}\boldsymbol{u}(t) = (\boldsymbol{A}-\boldsymbol{B}\boldsymbol{K})\boldsymbol{x}(t) = \boldsymbol{A}_{cl}\boldsymbol{x}(t), \tag{13}$$

where the closed-loop matrix, $\boldsymbol{A}_{cl}$, is included in Appendix A. The system will converge to its equilibrium states, $\boldsymbol{x}_0 = [0\ 0\ 0\ 0]^\top$, exponentially fast, when the closed-loop matrix, $\boldsymbol{A}_{cl}$, is Hurwitz. This occurs when all eigenvalues of $\boldsymbol{A}_{cl}$ have negative real part, i.e. $\Re(\lambda_i) < 0$. When the closed-loop matrix is Hurwitz, asymptotically stability of the origin is guaranteed. However, since the system is linear, the origin of (13) is globally exponential stable (GES).

Theorem 1. The closed-loop matrix, $\boldsymbol{A}_{cl}$, is Hurwitz. Hence, for the unperturbed system (13) globally exponentially stability of the origin is guaranteed.

Proof.

The quadratic Lyapunov candidate

$$V(\boldsymbol{x}) = \boldsymbol{x}^\top \boldsymbol{P}\boldsymbol{x}, \tag{14}$$

where $\boldsymbol{P}$ is a real symmetric positive definite matrix, $\boldsymbol{P} = \boldsymbol{P}^\top > 0$, is considered. The derivative of V along the trajectories of the linear system (13) is given by

$$\begin{aligned} \dot{V}(\boldsymbol{x}) &= \boldsymbol{x}^\top \boldsymbol{P}\dot{\boldsymbol{x}} + \dot{\boldsymbol{x}}^\top \boldsymbol{P}\boldsymbol{x} \\ &= \boldsymbol{x}^\top(\boldsymbol{P}\boldsymbol{A}_{cl} + \boldsymbol{A}_{cl}^\top \boldsymbol{P})\boldsymbol{x} = -\boldsymbol{x}^\top \boldsymbol{Q}\boldsymbol{x}, \end{aligned} \tag{15}$$

where $\boldsymbol{Q}$ is a symmetric matrix defined by

$$\boldsymbol{P}\boldsymbol{A}_{cl} + \boldsymbol{A}_{cl}^\top \boldsymbol{P} = -\boldsymbol{Q}. \tag{16}$$

Equation (16) is known as the Lyapunov equation. According to Khalil (2002), $\boldsymbol{A}_{cl}$ is Hurwitz if and only if for any positive definite symmetric matrix $\boldsymbol{Q} = \boldsymbol{Q}^\top > 0$, there exists a positive definite symmetric matrix $\boldsymbol{P}$ that satisfies the Lyapunov equation (16). In addition, $\boldsymbol{P}$ is an unique solution of (16). $\boldsymbol{P}$ and $\boldsymbol{Q}$ are chosen to be diagonal matrices with (p_1, p_2, p_3, p_4) and (q_1, q_2, q_3, q_4), respectively, on the main diagonal. A solution of (16) was found to be

$$p_1 = 1 \tag{17}$$
$$p_2 = C_{44}(A_{44} + I_{44}) \tag{18}$$
$$p_3 = \frac{a_{cl_{32}} C_{44}(A_{44} + I_{44})}{y_{cp} A_c p_0} \tag{19}$$
$$p_4 = \frac{a_{cl_{42}} C_{44}(A_{44} + I_{44})}{y_{cp} A_c p_0} \tag{20}$$
$$q_1 = 0 \tag{21}$$
$$q_2 = 2B_{44}C_{44} \tag{22}$$
$$q_3 = \frac{2p_3 K3}{K1} \tag{23}$$
$$q_4 = \frac{2p_4 K3}{K1}. \tag{24}$$

Since all terms in Equation (17)-(24) have positive interpretation, $\boldsymbol{P} = \boldsymbol{P}^\top > 0$ and $\boldsymbol{Q} = \boldsymbol{Q}^\top \geq 0$ when $a_{cl_{32}} > 0$ and $a_{cl_{42}} > 0$, which occurs for

$$k_{p_s} < \frac{y_{cp}\rho_{c0} A_c}{K2(A_{44} + I_{44})} \approx 0 \tag{25}$$
$$k_{p_p} > \frac{y_{cp}\rho_{c0} A_c}{K2(A_{44} + I_{44})} \approx 0, \tag{26}$$

where $K2(A_{44} + I_{44}) \gg y_{cp}\rho_{c0}A_c$. $\boldsymbol{Q}$ is not a positive definite matrix, therefore further analysis is necessary. By utilizing LaSalle's invariance principle, it can be proven that the origin is GES. From (21) it is seen that $q_1 = 0$, which implies that it can not be guaranteed that the roll angle approaches its origin when time goes to infinity. Hence, the state vector can be written $\boldsymbol{x} = [x_1\ 0\ 0\ 0]^\top$ when time approaches infinity. From (13) it is seen that $\dot{x}_2 = 0$ only if $x_1 = 0$. Therefore, $\boldsymbol{A}_{cl}$ is Hurwitz, and all states converge exponential fast to their origins. Hence, it is proved that by choosing the proportional gains for the commanded starboard and port vent valve positions according to (25) and (26), respectively, the roll angle, roll rate and air cushion pressures can not be driven unstable.

In order to validate that the wave-induced disturbances do not lead to an unstable system, a stability analysis of the perturbed closed-loop system is performed. The perturbed system, which includes disturbances, can be written

$$\dot{\boldsymbol{x}}(t) = \boldsymbol{A}\boldsymbol{x}(t) + \boldsymbol{B}\boldsymbol{u}(t) + \boldsymbol{E}\boldsymbol{w}(t) = \boldsymbol{A}_{cl}\boldsymbol{x}(t) + \boldsymbol{E}\boldsymbol{w}(t). \quad (27)$$

Since the perturbations $\boldsymbol{w}(t)$ are non-vanishing, it is not expected that the states converge to the origin. However, it can be shown that the solution, $\boldsymbol{x}(t)$, will be ultimately bounded by a small bound, b, if the perturbation term, $\boldsymbol{E}\boldsymbol{w}$, is small in some sense (Khalil, 2002).

Theorem 2. $\boldsymbol{x}(t)$ is ultimately bounded by b.

Proof.

By utilizing (14) and (27), equation (15) is written

$$\dot{V}(\boldsymbol{x}) = -\boldsymbol{x}^\top \boldsymbol{Q}\boldsymbol{x} + 2\boldsymbol{x}^\top \boldsymbol{P}\boldsymbol{E}\boldsymbol{w} < 0. \quad (28)$$

The inequality in equation (28) holds if the disturbance term fulfills

$$\|\boldsymbol{E}\boldsymbol{w}\| < \|\boldsymbol{T}\boldsymbol{x}\|, \quad (29)$$

where

$$2\boldsymbol{P}\boldsymbol{T} < \boldsymbol{Q}. \quad (30)$$

Then the perturbation term is bounded. The diagonal matrix $\boldsymbol{T}$ is determined according to

$$\boldsymbol{T} = \begin{bmatrix} 0 & 0 & 0 & 0 \\ 0 & \dfrac{B_{44}}{A_{44}+I_{44}} & 0 & 0 \\ 0 & 0 & \dfrac{K3}{K1} & 0 \\ 0 & 0 & 0 & \dfrac{K3}{K1} \end{bmatrix}. \quad (31)$$

From Lemma 9.2 in Khalil (2002) it follows that the solution of the perturbed system (27) is ultimately bounded by b, i.e. $\|\boldsymbol{x}(t)\| < b$.
Hence, when choosing appropriate controller gains and the vessel is subject to a roll wave excitation moment below a certain limit, the system states are ultimately bounded.
Note that the stability analysis does not take saturation of the control input into account. The control variable does have a strict upper bound, and as Figure 5 show, it can saturate. This can affect the performance of the system, but no stability problems have been encountered. However, further analysis of this will be a topic for further work.

4. MODEL TEST RESULTS

In order to validate the functionality of the longitudinally divided air cushion design and control system, multiple model tests were executed in the Towing Tank, NTNU, Trondheim. Bow, beam and quartering regular and irregular seas, with wave heights of 1 and 2 meters and various frequencies were applied to the model vessel to verify the overall performance of the roll damping control system.

Figure 5, 6 and 7 illustrate the commanded vent valve signals and the pressure and the roll angle response for regular beam seas with wave height of 1 meter and wave periods of 5, 6 and 8 seconds, respectively. Control is switched on after 42 seconds. From the figures it is seen that the control system is able to damp roll motions significantly for these environmental conditions. The roll angle is damped approximately $55-65$ % for waves with these periods. Note that the roll angle response characteristics for the wave period of 8 seconds, shown in Figure 7, differs from the response obtained for shorter periods. The reason for this is that the model scale vessel rolls with both its natural roll period and the wave period.

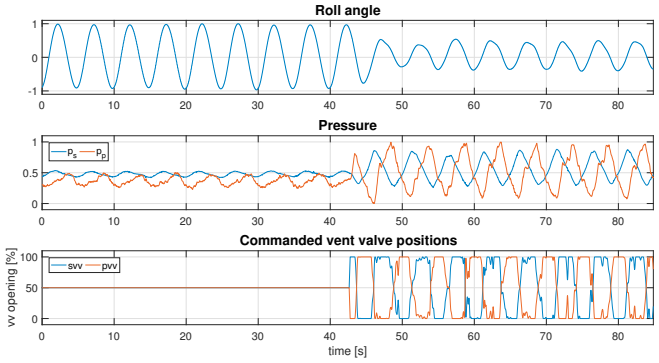

Fig. 5. Response for regular beam seas.
$H_w = 1\ m$ and $T_p = 5\ s$.

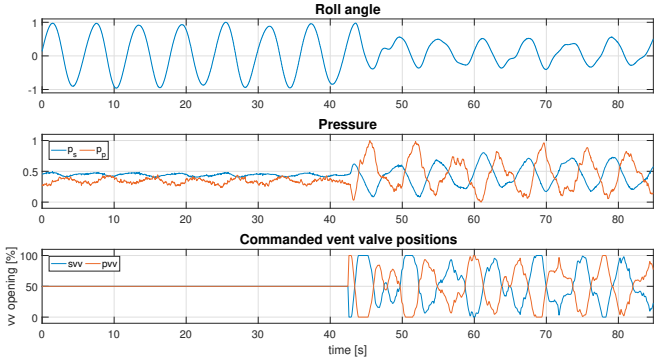

Fig. 6. Response for regular beam seas.
$H_w = 1\ m$ and $T_p = 6\ s$.

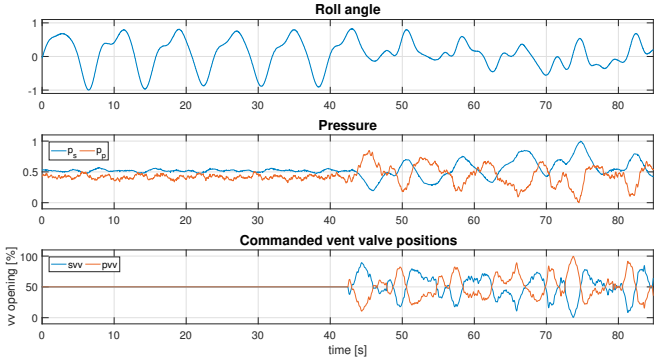

Fig. 7. Response for regular beam seas.
$H_w = 1\ m$ and $T_p = 8\ s$.

Irregular waves were applied to the vessel to validate the functionality of the roll damping control system in realistic environmental conditions. Figure 8 shows the results of 56

minute experiment in irregular waves with and without roll damping. Control is switched on after 28 minutes, where the controller gains, are kept constant during the entire control on sequence. The vessel was exposed to beam seas with significant wave height $H_s = 1\ m$, and peak period $T_p = 5\ s$. By using the MATLAB function `rms` the damping percentage was found to be 28.6 %.

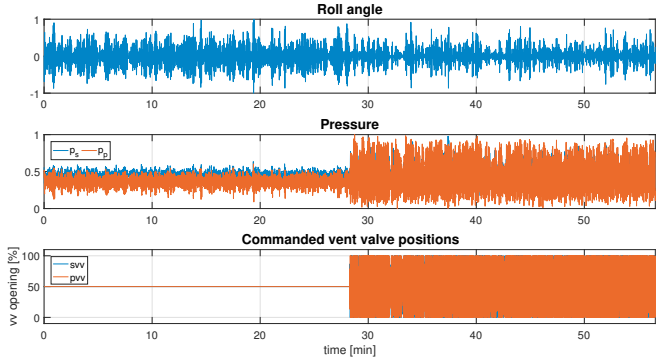

Fig. 8. Response for irregular beam seas. $H_s = 1\ m$ and $T_p = 5\ s$.

The overall roll damping performance of the control system is shown in Table B.1 and B.2. Figure 9 shows these results interpolated. Therefore, this figure gives an expected estimate of roll damping performance between the actual tested headings. The curves illustrate the roll damping percentages obtained for regular and irregular seas with various wave directions, heights and periods. The figure indicates that it is easier to damp roll motions for $H_w = 1\ m$ than $H_w = 2\ m$. Even though more roll damping occurs for smaller wave heights, the control system is able to damp $H_w = 2\ m$. The tendency is that more roll damping appears for longer wave periods and for bow and quartering seas than for beam seas. This makes sense: greater roll angular deflections appear for beam seas than for bow and quartering seas and the maximum achievable roll damping control moment is bounded due to the maximum and minimum cushion pressures.

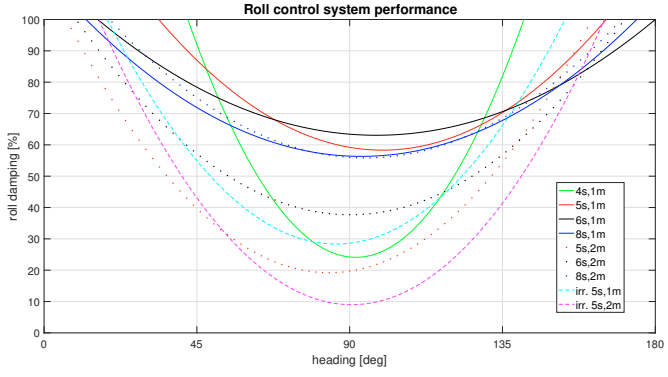

Fig. 9. Roll damping percentages for various wave directions, heights and periods.

5. CONCLUSION

A roll damping control system was implemented on a model scale surface effect ship with longitudinally split air cushions. Roll motions are damped significantly for various wave heights, periods and directions. Future studies will assess the effect of the split cushion on low speed manoeuvring properties of SES. Future work will include the application of the methodology developed to the design of an extended boarding control (for regulating roll, pitch and heave simultaneously) for a full scale SES.

ACKNOWLEDGEMENTS

A special thanks goes to Umoe Mandal for sharing data and being helpful and the Research Council of Norway MAROFF project 256442 for partly financing this project.

REFERENCES

Adams, J.D., Ernest, A.W., and Lewis, J.H. (1983). Design, development and testing of a digital ride control system for the xr-id surface effect ships; part i - classical control. Technical Report MD-AR-1180-1, Maritime Dynamics, Inc, Tacoma, Washington.

Auestad, Ø.F., Gravdahl, J.T., Perez, T., Sørensen, A.J., and Espeland, T.H. (2015). Boarding control system for improved accessibility to offshore wind turbines: Full-scale testing. *Control Engineering Practice*, 45, 207–218.

Bryn, H.E. and Tønnessen, J. (2017). *Nonlinear Modeling, Controller and Observer Design for Roll Damping on a Surface Effect Ship with Split Air Cushion*. Master's thesis, Department of Engineering Cybernetics, Norwegian University of Science and Technology.

Faltinsen, O.M. (2005). *Hydrodynamics of High-Speed Marine Vehicles*. Cambridge University Press, Cambridge, UK.

Fossen, T.I. (2011). *Handbook of Marine Craft Hydrodynamics and Motion Control*. John Wiley & Sons, UK.

Kaplan, P. and Davis, S. (1978). System analysis techniques for designing ride control system for ses craft in waves. In *Proceedings of the 5th Ship Contr. Syst. Symp.* Annapolis, Maryland, USA.

Khalil, H.K. (2002). *Nonlinear Systems*. Macmillan, New York, USA.

Perez, T. (2005). *Ship Motion Control: Course Keeping and Roll Reduction using Rudder and Fins. Advances in Industrial Control Series*. Springer-Verlag, London, UK.

Sørensen, A.J. and Egeland, O. (1995). Design of ride control system for surface effect ships using dissipative control. *Automatica*, 31, 183–199.

WindEurope (2017). *The European offshore wind industry key trends and statistics 2016*. WindEurope, Brussels, Belgium.

Appendix A. SYMBOLIC MATRICES

$$\boldsymbol{A} = \begin{bmatrix} 0 & \frac{1}{I_{44}+A_{44}} & 0 & 0 \\ -C_{44} & -\frac{B_{44}}{I_{44}+A_{44}} & -y_{cp}A_c p_0 & y_{cp}A_c p_0 \\ 0 & \frac{y_{cp}\rho_{c0}A_c}{K1(I_{44}+A_{44})} & -\frac{K3}{K1} & 0 \\ 0 & -\frac{y_{cp}\rho_{c0}A_c}{K1(I_{44}+A_{44})} & 0 & -\frac{K3}{K1} \end{bmatrix} \tag{A.1}$$

$$\boldsymbol{A}_{cl} = \begin{bmatrix} 0 & \frac{1}{I_{44}+A_{44}} & 0 & 0 \\ -C_{44} & -\frac{B_{44}}{I_{44}+A_{44}} & -y_{cp}A_c p_0 & y_{cp}A_c p_0 \\ 0 & \frac{y_{cp}\rho_{c0}A_c - K2k_{p_s}(A44+I_{44})}{K1(A_{44}+I_{44})} & -\frac{K3}{K1} & 0 \\ 0 & -\frac{y_{cp}\rho_{c0}A_c - K2k_{p_p}(A44+I_{44})}{K1(A44+I_{44})} & 0 & -\frac{K3}{K1} \end{bmatrix} \tag{A.2}$$

$$\boldsymbol{B} = \begin{bmatrix} 0 & 0 \\ 0 & 0 \\ \frac{K2}{K1} & 0 \\ 0 & \frac{K2}{K1} \end{bmatrix} \tag{A.3}$$

$$\boldsymbol{C} = \begin{bmatrix} 1 & 0 & 0 & 0 \\ 0 & \frac{1}{I_{44}+A_{44}} & 0 & 0 \\ 0 & 0 & 1 & 0 \\ 0 & 0 & 0 & 1 \end{bmatrix} \tag{A.4}$$

$$\boldsymbol{E} = \begin{bmatrix} 0 & 0 & 0 \\ 1 & 0 & 0 \\ 0 & \frac{\rho_{c0}}{K1} & 0 \\ 0 & 0 & \frac{\rho_{c0}}{K1} \end{bmatrix} \tag{A.5}$$

Appendix B. TABLES

Table B.1. Roll damping percentages for regular seas.

Wave direction	$H_w = 1\ m$				$H_w = 2\ m$			
	4s	5s	6s	8s	4s	5s	6s	8s
45°	92.0 %	87.0 %	71.5 %	71.9 %	N.A.	39.7 %	57.2 %	75.0 %
90°	24.2 %	59.2 %	63.4 %	59.0 %	N.A.	19.7 %	37.7 %	47.0 %
135°	81.9 %	70.3 %	70.6 %	67.8 %	73.0 %	54.4 %	56.9 %	68.5 %

Table B.2. Roll damping percentages for irregular seas with $T_p = 5\ s$.

Wave direction	$H_s = 1\ m$	$H_s = 2\ m$
45°	54.9 %	43.1 %
90°	28.6 %	9.0 %
135°	66.2 %	41.4 %